

# Development of Electrospun Polymer Nanofiber Membrane Based on PAN/PVDF as a Supercapacitor Separator

Nasikhudin<sup>1,2,\*</sup>, Fina Nur Azizah<sup>1</sup>, Ulwiyatus Sa'adah<sup>1</sup>, Markus Diantoro<sup>1,2</sup>, Hartatiek<sup>1</sup> & Ramesh T. Subramaniam<sup>3</sup>

<sup>1</sup>Department of Physics, Faculty of Mathematics and Natural Science, State University of Malang, Jalan Semarang No. 5 Malang 65145, Indonesia

<sup>2</sup>Center of Advanced Materials for Renewable Energy, CAMRY, State University of Malang, Jalan Semarang No. 5 Malang 65145, Indonesia

<sup>3</sup>Department of Physics, Faculty of Natural Science, Universiti Malaya, Jalan Profesor Diraja Ungku Aziz No. 13 Kuala Lumpur 50603, Malaysia

Corresponding author: nasikhudin.fmipa@um.ac.id

## Abstract

Among various types of energy storage, the supercapacitor is regarded as the most promising device due to its long cycling life, good cycling stability, and high power density. A supercapacitor is generally composed of electrodes, electrolytes, and a separator. The separator is one of the most important components, serving to prevent internal short circuits between the anode and the cathode. Herein, a nanostructured-based separator in a PAN/PVDF nanofiber scheme is introduced for improving the electrochemical performance of the supercapacitor. Briefly, the membranes were produced via the electrospinning technique. All of the raw materials were blended in various compositions of PVDF for optimization purposes. Fourier transform infrared spectroscopy (FTIR) and scanning electron microscopy (SEM) were carried out to identify the microstructure of the nanofibers. The electrochemical properties of the membrane were measured using galvanostatic charge-discharge (GCD). Based on GCD, it was shown that the PAN/PVDF 20 wt% membrane exhibited the optimum gravimetric capacitance at  $54.104 \text{ Fg}^{-1}$  as evidenced by a high porosity percentage. Thus, the PAN/PVDF nanofiber has good potential as a separator for application in supercapacitors.

**Keywords:** *membrane; nanofiber; separator; supercapacitor; PAN/PVDF.*

## Introduction

In this modern era, the demand for electrical energy is increasing rapidly to support human life. The increasing consumption of fossil fuels and environmental problems in the current era are triggering exploration of sustainable energy sources and more effective energy storage techniques [1]. The development of energy storage in the world of battery-based research is very rapid, and the existence of batteries is very important in system planning and operations in everyday life. However, their use in a sustainable manner harms the earth, because the materials used in batteries so far are still based on lithium-ion, which is considered environmentally unfriendly.

A renewable energy storage device that is currently attracting great attention is the supercapacitor. Supercapacitors are a very attractive alternative storage system with almost the same properties as conventional capacitors, which can act as batteries [2]. The capacitance of supercapacitors is higher than that of conventional capacitors, while their life cycle is longer than that of batteries [3]. Other advantages of supercapacitors include high power density, fast charge-discharge rate [4], large density, environmental friendliness, and large storage capacity [5].

One of the important components of a supercapacitor is the separator, which is inserted between two electrodes to prevent direct electron transfer, avoid short circuits, and regulate the rate and amount of ion mobility [5,6]. Nanostructured separators potentially increase capacitance in supercapacitor systems due to their high specific surface area and fast electron mobility. Several researchers have revealed that the separator can be used as a

determinant of supercapacitor performance [7,8]. One of the factors that affect the performance of the separator is related to the thickness of the membrane (or a thin flexible structure in general) [9], and its porosity, which can affect the length of time the ions pass through it during the charge-discharge state, while an optimal thickness can improve the electrochemical performance of supercapacitors [10]. However, the separator only acts as a membrane and a liquid electrolyte solution is still employed as an intermediary for electron mobility in the supercapacitor. Since the utilization of liquid electrolytes allows leakage and corrosion, also unstable in supercapacitors, so its optimization is required to avoid the risk [11,12].

Nowadays, membranes play an important role in the development of technology, including membrane bioreactors for processing wastewater treatment [13], membrane oxygenators for extracorporeal blood oxygenation [14], and chemical precipitation-ultrafiltration for waste brine regeneration [15]. One of the most widely used techniques for producing membranes is electrospinning. Electrospinning is a unique spinning technique that applies electrostatic forces to produce a fine membrane from a polymer solution [16]. This technique is one way to produce very long one-dimensional nanofiber structure separators with a simple procedure [17,18]. Membranes produced from this method are very light and have flexible properties with a high surface area and porosity [17,19], high chemical and mechanical resistance properties [7], and good electrochemical performance when compared to commercial separators. Some commercial synthetic polymers that have been developed as host polymers are polyethylene (PE), polypropylene (PP), polyvinylidene fluoride (PVDF), polymethyl methacrylate (PMMA), polyacrylonitrile (PAN), and polyethylene oxide (PEO) [20]. Synthetic fibers requiring high expenses and natural fibers have been studied as potential reinforcement in composite applications [21]. In general, thermoplastic polymers possess unique properties (physical, thermal, and electrical) that make them suitable for a wide range of applications since they are light-weight, inexpensive, and durable [22]. Several studies have reported that the application of polyvinylidene fluoride (PVDF) based nanofiber separators synthesized using electrospinning showed optimal supercapacitor system performance [17,23,24]. Among the various polymers, PVDF exhibits high electrochemical stability and good electrical properties that have potential for supercapacitor applications. However, this polymer has low flexibility due to its high crystallinity [17], so the addition of a material is required to strengthen the mechanical properties of PVDF. Polyacrylonitrile (PAN) shows good resistance to oxidative degradation and chemical stability, and high oxidative stabilization even at high temperatures [25]. So far, the manufacture of PAN/PVDF nanofiber composite membranes for supercapacitor application has not been reported. The optimization of the membrane's microstructures and their performance will be discussed in detail.

## Materials and Methods

### Materials

To prepare the electrospinning solution, the materials used were polyacrylonitrile (PAN, MW = 150,000 g/mol), polyvinylidene fluoride (PVDF, MW = 180,000 g/mol) and N,N-dimethylformamide (DMF) were purchased from Sigma-Aldrich. Activated carbon (AC, CGC, Bangkok, Thailand) and carbon black (CB, Imerys, La Hulpe, Belgium) were used as electrode materials. Tetraethylammonium tetrafluoroborate (Et<sub>4</sub>NBF<sub>4</sub>, Gelon, Shandong, China) was applied for the electrolytes of the device.

### Preparation of PAN/PVDF Nanofiber Membranes and Fabrication of Supercapacitor

Each electrospun solution used was 5 mL, composed of 8 wt% total polymers (PAN+PVDF) dissolved in 92 wt% solvents of DMF. First, PAN of various masses of 0.4, 0.36, 0.32, 0.28, and 0.24 g were dissolved into DMF using a magnetic stirrer at 80 °C for 1 hour. Then, various amounts of PVDF of 0, 10, 20, 30, and 40 wt% (0, 0.04, 0.08, 0.12, and 0.16 g, respectively) were added to the PAN:DMF solution and stirred for 2 hours. The polymer solutions were sonicated for 1 hour to produce a homogeneous solutions. The final solutions were allowed to mix in a magnetic stirrer for 24 hours. The homogeneous PAN/PVDF composite solution was electrospun to obtain a PAN/PVDF nanofiber membrane using electrospinning with a high voltage of 10 kV. The fiber in this process collected on the aluminum foil substrate was then annealed in the oven at 75 °C for 5 hours.

The supercapacitor in this study was prepared using the sandwiching method. The electrodes used were AC-CB electrodes, which were placed in the middle of a glass slide and separated by a four-layer PAN/PVDF nanofiber

separator membrane. The electrolyte applied in this system was tetraethylammonium tetrafluoroborate ( $\text{Et}_4\text{NBF}_4$ ) dissolved in acetonitrile.

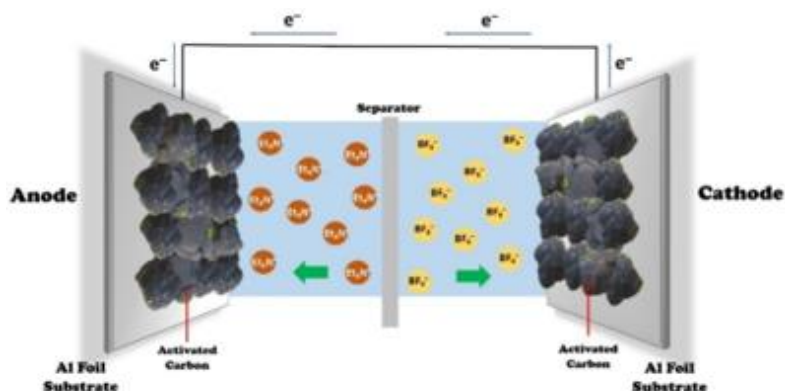


**Figure 1** Schematic of a symmetrical supercapacitor.

## Characterization

The functional group of the PAN/PVDF nanofiber membrane was characterized by fourier transform infrared (FTIR) spectroscopy, which was observed at a wave numbers from 4000 to 500  $\text{cm}^{-1}$  using a Shimadzu, type IRPrestige 21. The morphology, fiber diameter distribution, and porosity of the PAN/PVDF nanofiber membrane were characterized by scanning electron microscopy (SEM) using an Inspect-S50 FEI.

The porosity of the PAN/PVDF nanofiber membrane was also tested using the n-butanol absorption method. The percentage of membrane porosity can be determined based on the calculation of the membrane mass before and after immersion in n-butanol for 2 hours using Eq. (1):

$$\text{Porosity (\%)} = \frac{w_i - w_0}{w_0} \quad (1)$$

where,  $w_0$  is the mass of the membrane before immersion, while  $w_i$  is the mass of the membrane after immersion.

The electrochemical properties of the PAN/PVDF nanofiber separator membrane were studied based on the supercapacitor's specific capacitance, which was calculated using galvanostatic charge-discharge (GCD) test data. Measurements were carried out using a GCD Newar BTS 4000 instrument. From the GCD test, the calculation of specific capacitance  $C(\text{Fg}^{-1})$ , energy density  $E(\text{Whkg}^{-1})$ , and power density  $P(\text{Wkg}^{-1})$ , which were calculated using Eqs. (2) to (4) [26,27]:

$$C = \frac{4I\Delta t}{m\Delta V} \quad (2)$$

$$E = \frac{1}{8} \frac{C\Delta V^2}{3.6} \quad (3)$$

$$P = \frac{E \times 3600}{\Delta t} \quad (4)$$

where  $I$  is the discharge current (mA),  $m$  is the electrode mass (g),  $\Delta V$  is the potential difference (V), and  $t$  is the discharge time (s).

## Results and Discussion

### Functional Group of Nanofiber Membrane

The IR spectra of the PAN/PVDF nanofiber membranes is depicted in Figure 2. The obtained characteristics of each peak are presented in Table 1.

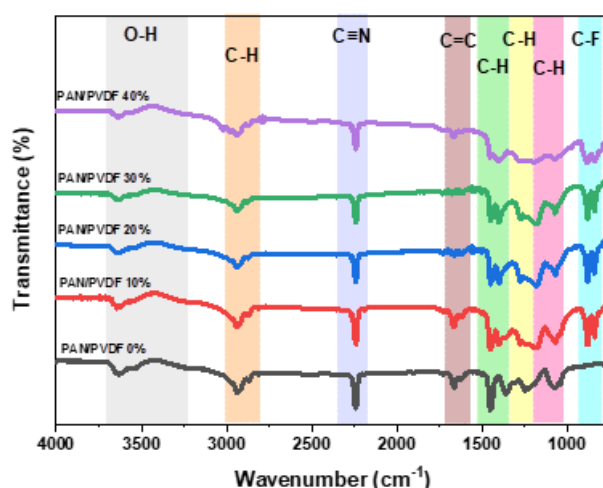


**Figure 2** IR spectra of PAN /PVDF nanofiber membranes at five composition variations.

**Table 1** Comparison of the IR spectra of the PAN/PVDF nanofiber membranes.

Wave Number (cm <sup>-1</sup> )			Bonding Characteristics
PAN nanofiber	PAN/PVDF Nanofiber	Reference	
-	880.91	~880	C-F stretching vibration [28,26]
1073.90	1073.90	~1190-1390	Methylene (C-H) group [29]
1248.75	1272.70	~1220-1270	Aliphatic CH (CH, CH <sub>2</sub> , CH <sub>3</sub> ) group vibration [30,31]
1363.39	-	~1350-1380	Aliphatic CH (CH, CH <sub>2</sub> , CH <sub>3</sub> ) group vibration [30,31]
-	1405.47	~1405	CF <sub>2</sub> symmetrical stretching groups [28]
1451.91	1449.73	~1450-1560	Aliphatic C-H (CH, CH <sub>2</sub> , CH <sub>3</sub> ) group vibration [30-33]
1666.5	1666.5	~1631-1668	C=N stretching vibration [30]
2243.47	2245.64	~2240 -2361.4	C≡N nitrile group stretching vibration [34-37]
2939.26	2939.26	~2870-2940	Stretching vibration C-H (CH, CH <sub>2</sub> , CH <sub>3</sub> ) group [35,36]
3632.15	3645,21	~3200-3700	O-H Stretching vibration [36,38]

The absorption with high intensity at wave number of 2243, 47 cm<sup>-1</sup> was observed. The functional group is related to the C≡N stretching vibration of the nitrile group. However, the intensity decreased significantly with increasing PVDF concentration [23,40].

The characteristics of each peak in the IR PAN spectrum before and after being composited with the PVDF polymer materials are presented in Table 1. Functional groups with the C≡N stretching vibration nitrile group, the aliphatic group C-H (CH, CH<sub>2</sub>, CH<sub>3</sub>) vibration, and the stretching vibration C=O are a characteristic of the PAN membrane functional group [39]. Meanwhile, in the IR PAN/PVDF spectrum, it was shown that there was a functional group of the PAN, but there was a shift in the band vibration in one of the functional groups. Wave number 1363.39 cm<sup>-1</sup> with an aliphatic C-H (CH, CH<sub>2</sub>, CH<sub>3</sub>) vibration group has a peak shift at a wave number of 1405.47 cm<sup>-1</sup> with a CF<sub>2</sub> symmetrical stretching functional group. In the IR PAN/PVDF spectrum there is also a new peak that appears at wave number 880.91 cm<sup>-1</sup>, which indicates the C-F stretching vibration functional group. The existence of a shift and the appearance of new peaks in the IR spectrum of the PAN/PVDF nanofiber composite membrane informed that there was a PVDF polymer in the PAN polymer mixture. These two peaks are characteristic of the PVDF functional group [28]. Surface functional groups—O-containing and N-containing groups—in the IR PAN/PVDF spectrum are the important functional groups that affect the performance of the

separator. These functional groups can significantly enhance the total capacitance through additional Faradaic reactions called the pseudo-capacitance effect [17].

### Nanofiber Membrane Morphology

The morphology, diameter, porosity, and pore size of the PAN/PVDF nanofiber membranes were characterized using a scanning electron microscope. The SEM images were then analyzed using the ImageJ and the Origin software packages to obtain a histogram of the fiber diameter distribution.

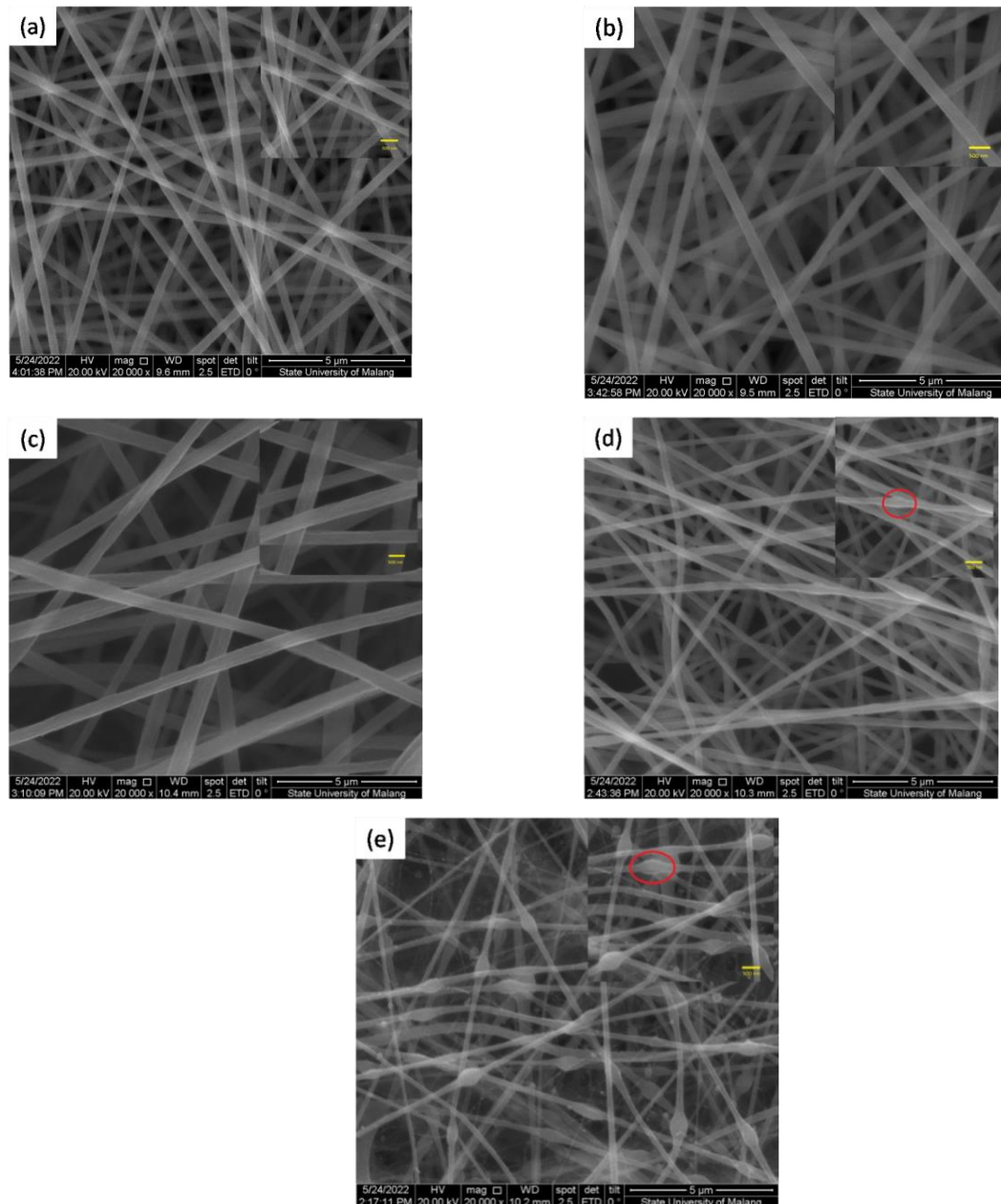


**Figure 3** Surface morphology of PAN/PVDF nanofiber membranes and fiber diameter distribution: (a) 0, (b) 10, (c) 20, (d) 30, and (e) 40 wt% PVDF.

Figure 3 is a SEM image of the PAN/PVDF nanofiber membrane synthesized with several concentrations of PVDF (0, 10, 20, 30, and 40 wt%) observed at a magnification of 20,000 times. The surface morphology of the SEM images show smooth nanofibers without beads at low PVDF concentrations, but in contrast, beads were observed with increasing PVDF concentrations. The appearance of these beads is a consequence of the low

viscosity due to an increase in agglomeration of the PVDF particles, so it is difficult to maintain the elongation of the liquid in an electrospinning jet [40]. The optimum PVDF concentration in the PAN/PVDF electrospinning solution was found at a PVDF concentration of 20 wt%.

**Table 2** Average diameter, porosity, and pore size of PAN/PVDF nanofiber membranes.

Sample	Diameter (nm)	$\emptyset$ (%)	Pore size (nm)
PAN/ PVDF 0%	337.1 $\pm$ 4.0	59.27	365.1
PAN/ PVDF 10%	389.7 $\pm$ 9.9	62.94	482.0
PAN/ PVDF 20%	537.8 $\pm$ 11.2	70.55	1059.9
PAN/ PVDF 30%	261.4 $\pm$ 4.7	66.64	462.2
PAN/ PVDF 40%	240.9 $\pm$ 7.9	67.26	579.5
Whatman filter paper		63.77	

Based on Table 2, it can be seen that the fiber diameter size increased with the increase of the PVDF polymer concentration. The fiber diameter increased from 240.9 nm to 537.8 nm. Uniform fibers were formed due to an increase in the polymer concentration in the electrospinning jet and also interactions between polymer chains in the solution. Thus, with increasing PVDF concentration, the average fiber diameter also increases [41]. The largest average diameter was obtained on the PAN/PVDF nanofiber separator membrane with a PVDF concentration of 20 wt%, i.e., (537.8  $\pm$  11.2) nm. Then it decreased at a concentration of 30 wt% PVDF (261.4  $\pm$  4.7) nm. The nanofiber diameter size in this experiment was 100 to 500 nm [42].

The SEM image in Figure 3 was also analyzed using the Origin software to obtain the percentage of nanofiber membrane porosity. Good porosity can increase the surface area of the pores, affecting the absorption of nanofiber membranes. Table 2 shows that the maximum porosity obtained from the PAN/PVDF nanofiber membrane with a PVDF concentration of 20 wt% was 70.55%, meaning that good absorption of the separator membrane electrolyte occurred at this concentration. Table 2 also shows the percentage of Whatman filter paper porosity, but the percentage of porosity was still below the maximum porosity percentage of the PAN/PVDF nanofiber membrane obtained.

The porosity is influenced by the pore size. The larger the pore size, the greater the absorption ability of a nanofiber membrane. A nanofiber separator membrane with a large pore size will be very useful for the absorption of large amounts of electrolytes [43]. The ideal pore size for the separator is  $< 1 \mu\text{m}$  [44]. In this study, the electrolyte  $\text{Et}_4\text{NBF}_4$  with an  $\text{Et}_4\text{N}^+$  ion diameter of 0.343 nm was used, while the  $\text{BF}_4^-$  ion had a diameter of 0.229 nm [45]. Based on the resulting pore size, which was in the range of 365.1 to 1059.9 nm, it means that the rate and mobility of ions could run smoothly.

Another efficient method for measuring the porosity of nanofiber membranes is to use the n-butanol absorption method [41]. The porosity is a percentage of the pore volume to the total membrane volume [46]. Based on calculations using Eq. (1), the results of the porosity of the PAN/PVDF nanofiber membrane based on the n-butanol method are presented in Table 3.

**Table 3** Porosity percentage of PAN/PVDF nanofiber membrane based on the n-butanol absorption method.

Sample	$\emptyset$ (%)
PAN/PVDF 0%	185.18
PAN/PVDF 10%	188.55
PAN/PVDF 20%	197.53
PAN/PVDF 30%	162.55
PAN/PVDF 40%	128.09
Whatman filter paper	90.53

Table 3 shows the porosity percentage using the n-butanol absorption method appropriate with the results of the surface porosity of the SEM images analyzed using the Origin software. The porosity plays an important role in supercapacitor separators. Separators with a multi-pore structure can reduce mechanical stability. On the other hand, a limited number of pores will also affect the accessibility of the electrolytes at the supercapacitor electrode [47]. The ability of the nanofiber membrane to absorb is referred to as the swelling ability or can be interpreted as the ability to increase the size of the nanofiber diameter due to the absorption process.

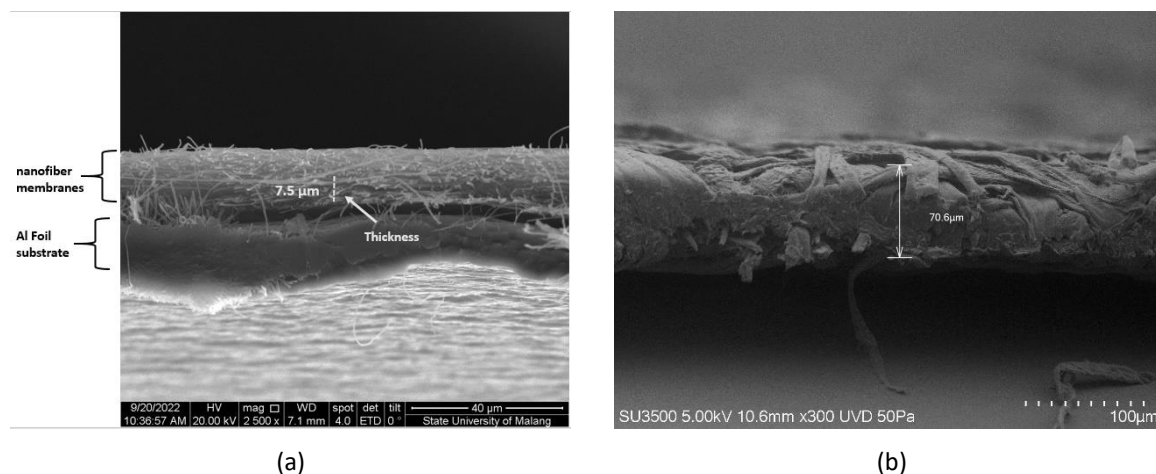


**Figure 4** Cross-section of separator: (a) PAN/PVDF membrane 20 wt% nanofibers, (b) Whatman filter paper.

To determine the thickness of the separator obtained by SEM cross-section test is shown in Figure 4. Figure 4 (a) is the 20 wt% PAN/PVDF nanofiber membrane cross-section, which was selected based on the optimum results of the nanofiber membrane in each test, while Figure 4 (b) is a cross-section Whatman filter paper separator. Based on Figure 4, the thickness of the 20 wt% PAN/PVDF nanofiber membrane is much thinner ( $7.5 \mu\text{m}$ ) when compared to the Whatman filter paper separator ( $70.6 \mu\text{m}$ ). The thickness of the separator is an important factor for the capacitance in the electrochemical properties of supercapacitors. In addition, the separator must be thin, porous, and have a great dielectric substance to facilitate electron ion transfer [48], so a separator that is too thick will only provide long ion diffusion distances [49].

### Electrochemical Properties of Nanofiber Separator Membrane Supercapacitors

Symmetrical supercapacitors use activated carbon (AC) – carbon black (CB) electrodes. Activated carbon is the most popular material and has been widely used as a conventional supercapacitor electrode material because of its high surface area, wide availability, and inexpensiveness [50]. Carbon black is added as a suitable conductive additive to increase the capacitance. The electrochemical properties of this supercapacitor were carried out using a galvanostatic charge-discharge (GCD) test. The correlation between voltage (V) and time (s) is shown in Figure 5.



**Figure 5** Supercapacitor charge-discharge: (a) PAN/PVDF nanofiber separator membrane, (b) comparison of commercial separators.

Based on Figure 5(a), the PAN/PVDF nanofiber separator membrane with a PVDF concentration of 20% showed a longer discharge time than the other concentration variations, at almost 300 seconds. Meanwhile, comparing the curve to that of commercial separators, a Whatman filter paper separator in this case, showed an increase in discharging time. The supercapacitor gravimetric capacitance was calculated using Eq. (2). The following table presents the results of calculating the capacitance, energy density, and power density.

Table 4 and Figure 6 show that increasing the concentration of PVDF causes an increase in the gravimetric capacitance of supercapacitors based on PAN/PVDF nanofiber membrane separators. The curve in Figure 6 also informs that the performance of supercapacitors based on PAN/PVDF nanofiber separator membranes reached its optimum limit at a PVDF concentration of 20% with a gravimetric capacitance of  $54.104 \text{ Fg}^{-1}$ . However, starting with a PVDF concentration of 30%, there was a decrease in performance, which was suspected of increasing the PVDF's crystallinity, causing a decrease in the conductivity of the PAN/PVDF nanofiber composite separator membrane [51]. If the optimum supercapacitor performance is indicated by the PAN/PVDF nanofiber separator membrane with a PVDF concentration of 20%, the results are in accordance with the tests with a large diameter, porosity, and pore size of the PAN/PVDF nanofiber membrane, which also achieved optimum performance at this concentration. In this condition, the amount of electrolyte that can be absorbed in the membrane will increase. Increasing the electrolytes is effectively an ion transfer mechanism. In another result, a PVDF of 30% and 40% showed decreasing performance. This may be caused by a decreased porosity and pore size when enhancing the concentration.

**Table 4** Values of gravimetric capacitance, energy density, and power density of supercapacitors based on PAN/PVDF nanofiber separator membranes.

Sample	$C(\text{Fg}^{-1})$	$E(\text{Whkg}^{-1})$	$P(\text{Wkg}^{-1})$
PAN/PVDF 0%	37.506	0.690	36.720
PAN/PVDF 10%	38.673	0.781	37.991
PAN/PVDF 20%	54.104	1.143	38.827
PAN/PVDF 30%	46.91	1.010	39.512
PAN/PVDF 40%	35.501	0.641	36.055

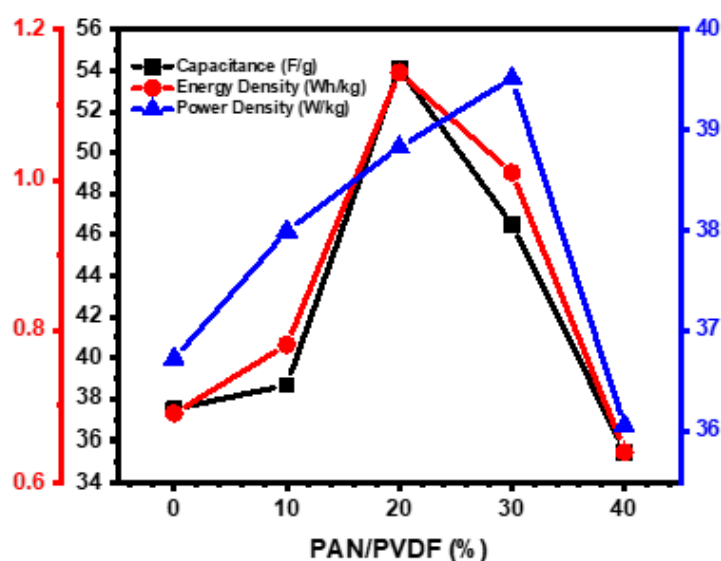


**Figure 6** Graph of specific capacitance, energy density, and power density of supercapacitor based on PAN/PVDF nanofiber separator membrane.

**Table 5** Comparison of gravimetric capacitance values, energy density, and power density of PAN/PVDF nanofiber membrane separator-based supercapacitors with commercial separators.

Sample	$C(\text{Fg}^{-1})$	$E(\text{Whkg}^{-1})$	$P(\text{Wkg}^{-1})$
PAN/PVDF 20%	54.104	1.143	38.827
Whatman filter paper	50.416	1.200	41.148

Table 5 compares the gravimetric capacitance of the 20% PAN/PVDF nanofiber separator membrane with the Whatman filter paper separator. The results of this comparison show that the gravimetric capacitance of the



20% PAN/PVDF nanofiber separator membrane was higher than that of the Whatman filter paper separator. However, the energy density of PAN/PVDF 20% was almost the same as that of the Whatman filter paper separator. The energy density is influenced by the ionic conductivity of the electrolyte membrane. Using 1 M electrolyte  $\text{Et}_4\text{NBF}_4$  with  $\text{Et}_4\text{N}^+$  ions to increase ionic conductivity has been reported [20]. Diantoro et al. [52] used coconut shell-based activated carbon (ACCS) electrodes, polyethylene separators, and 1 M electrolyte  $\text{Et}_4\text{NBF}_4$ . It revealed that ACCS supercapacitors with activation temperatures of 500 and 700 °C achieve a specific capacitance of  $46.733 \text{ Fg}^{-1}$ . When compared with this study, the capacitance values of the 20% PAN/PVDF nanofiber separator membrane was higher. From all these studies, the values of capacitance, energy density and power density in this study indicates that the optimum PAN/PVDF nanofiber separator membrane at a concentration of 20% was almost equivalent to that of a commercial separator.

## Conclusion

Characterization of the PAN/PVDF membrane showed a shift and the addition of new peaks in the spectrum, indicating the presence of PVDF polymer material in the PAN polymer mixture. In the SEM characterization, the surface morphology showed smooth nanofibers without beads at low PVDF concentrations but otherwise beads were observed with increasing PVDF concentrations. The increasing concentration of PVDF also affects an increase of the diameter of the resulting fiber, which ranged from 240.9 to 537.8 nm. Thus, it also affects the nanofiber membrane porosity percentage. The optimum porosity percentage was obtained at a PVDF concentration of 20 wt%, at 70.55%. In testing the performance of supercapacitors using a PAN/PVDF nanofiber membrane as a separator, it was shown that the results could reach its optimum limit at a PVDF concentration of 20%, with a gravimetric capacitance value of  $54.104 \text{ Fg}^{-1}$ .

## Acknowledgement

The authors would like to thank you for the financial support through a Non-APBN Funding Sources Research grant from the State University of Malang for the Implementation Year 2022 [Contract No. 18.5.60/UN32/KP/2022].

## References

- [1] Chai D., Huang, H., Wang, D., Liu, B., Wang, L., Liu, Y., Li, Q. & Wang, T., *High-Performance Supercapacitor Electrode Based on the Unique ZnO@ Co3O4 Core/Shell Heterostructures on Nickel Foam*, ACS Applied Materials & Interfaces, **6**(18), pp. 15905-15912, Sept. 2014.
- [2] Hu, M., Li, Z., Li, G., Hu, T., Zhang, C. & Wang, X., *All-Solid-State Flexible Fiber-Based MXene Supercapacitors*, Advanced Materials Technologies, **2**(10), 1700143, Oct. 2017.
- [3] Widiatmoko, P., Devianto, H., Nurdin, I. & Yandra, R.E., *The Effect of Carbon Nanotube Composite Addition on Biomass-Based Supercapacitor*, Journal of Engineering and Technological Sciences, **48**(5), pp. 597-613, Nov. 2016.
- [4] Miao, Y.E., Yan, J., Huang, Y., Fan, W. & Liu, T., *Electrospun Polymer Nanofiber Membrane Electrodes and an Electrolyte for Highly Flexible and Foldable All-Solid-State Supercapacitors*, Royal Society of Chemistry Advances, **5**(33), pp. 26189-26196, 2015.
- [5] Rohmawati, L., Setyarsih, W. & Nurjannah, T., *Variation Sweep Rate Cyclic Voltammetry on the Capacitance Electrode Activated Carbon/PVDF with Polymer Electrolyte*, Journal of Physics: Conference Series, **997**, 012003, Mar. 2018.
- [6] Taer, E. Sugianto, Sumantre, M.A., Taslim, R., Iwantono, I., Dahlan, D. & Deraman, M., *Eggs Shell Membrane as Natural Separator for Supercapacitor Applications*, Advanced Materials Research, **896**, pp. 66-69, Feb. 2014.
- [7] Szubzda, B., Szmaja, A., Ozimek, M. & Mazurkiewicz, S., *Polymer Membranes as Separators for Supercapacitors*, Applied Physics A Materials Science & Processing, **117**(4), pp. 1801-1809, Dec. 2014.
- [8] Liu, X., Marlow, M.N., Cooper, S.J., Song, B., Chen, X., Brandon, N.P. & Wu, B., *Flexible All-Fiber Electrospun Supercapacitor*, Journal of Power Sources, **384**, pp. 264-269, Apr. 2018.

- [9] Prasetyo, I., Desendra, G., Anwar, K. & Agusta, M.K., *Noise Attenuation of a Duct-resonator System Using Coupled Helmholtz Resonator - Thin Flexible Structures*, Journal of Engineering and Technological Sciences, **53**(6), 210605, Dec. 2021.
- [10] Islam, M.A., Ong, H.L., Villagracia, A.R., Halim, K.A.A., Ganganboina, A.B. & Doong, R.A., *Biomass-Derived Cellulose Nanofibrils Membrane from Rice Straw as Sustainable Separator for High Performance Supercapacitor*, Industrial Crops and Products, **170**, 113694, Oct. 2021.
- [11] Liu, X., Shi, C., Zhai, C., Cheng, M., Liu, Q. & Wang, G., *Cobalt-Based Layered Metal-Organic Framework as an Ultrahigh Capacity Supercapacitor Electrode Material*, ACS Applied Materials and Interfaces, **8**(7), pp. 4585-4591, 2016.
- [12] Cheikh, Z.B., Kamel, F.E., Lavallee, O.G., Soussou, M.A., Vizireanu, S., Achour, A. & Khirouni, K., *Hydrogen Doped BaTiO<sub>3</sub> Films as Solid-State Electrolyte for Micro-Supercapacitor Applications*, Journal of Alloys and Compounds, **721**, pp. 276-284, Oct. 2017.
- [13] Chiemchaisri, C., Chiemchaisri, W., Dachsrijan, S. & Saengam, C., *Coliform Removal in Membrane Bioreactor and Disinfection during Hospital Wastewater Treatment*, Journal of Engineering and Technological Sciences, **54**(4), 220401, Jul. 2022.
- [14] Ratnaningsih, E., Aryanti, P.T.P., Himma, N.F., Wardani, A.K., Khoiruddin, K., Kadja, G.T.M., Prasetya, N. & Wenten, I.G., *Membrane Oxygenator for Extracorporeal Blood Oxygenation*, Journal of Engineering and Technological Sciences, **53**(5), 210502, Oct. 2021.
- [15] Wenten, I.G., Khoiruddin, K., Hakim, A.N., Aryanti, P.T.P. & Rova, N., *Long-Term Performance of a Pilot Scale Combined Chemical Precipitation-Ultrafiltration Technique for Waste Brine Regeneration at Chevron Steam Flooding Plant*, Journal of Engineering and Technological Sciences, **52**(4), pp. 501-513, Jul. 2020.
- [16] Nasikhudin, Ismaya, E.P., Diantoro, M., Kusumaatmaja, A. & Triyana, K., *Preparation of PVA/TiO<sub>2</sub> Composites Nanofibers by using Electrospinning Method for Photocatalytic Degradation*, IOP Conference Series: Materials Science and Engineering, **202**, 012011, May 2017.
- [17] Asmatulu, R. & Jabbaria, A., *Synthesis and Characterization of PVdF/PVP-Based Electrospun Membranes as Separators for Supercapacitor Applications*, Journal of Material Science and Technology Research, **2**(2), pp. 43-51, Jul. 2016.
- [18] Chen, K., Wang, Q., Niu, Z. & Chen, J., *Graphene-based Materials for Flexible Energy Storage Devices*, Journal of Energy Chemistry, **27**(1), pp. 12-24, 2018.
- [19] Nasikhudin, Diantoro, M., Kusumaatmaja, A. & Triyana, K., *Preparation of PVA/Chitosan/TiO<sub>2</sub> Nanofibers Using Electrospinning Method*, AIP Conference Proceedings, **1755**, 150002, 2016.
- [20] Ndruru, S.T.C.L., Wahyuningrum, D., Bundjali, B. & Arcana, I.M., *Preparation and Characterization of Biopolymer Electrolyte Membranes Based on Liclo<sub>4</sub>-Complexed Methyl Cellulose as Lithium-Ion Battery Separator*, Journal of Engineering and Technological Sciences, **52**(1), pp. 28-50, Feb. 2020.
- [21] Laziz, A.A., Mazlan, N., Yusoff, M.Z.M. & Ariff, A.H.M., *Investigation of Alkaline Surface Treatment Effected on Flax Fibre Woven Fabric with Biodegradable Polymer Based on Mechanical Properties*, Journal of Engineering and Technological Sciences, **52**(5), pp. 677-690, Sep. 2020.
- [22] Sultana, S., Sarker, M.K.U., Islam, Z. & Islam, M.S., *Comparative Analysis of Compression Molded Products of Recycled Waste Poly (Vinyl Chloride) and Virgin Poly (Vinyl Chloride) Fill Material*, Journal of Engineering and Technological Sciences, **54**(4), 220412, Jul. 2022.
- [23] He, T., Jia, R., Lang, X., Wu, X. & Wang, Y., *Preparation and Electrochemical Performance of PVdF Ultrafine Porous Fiber Separator-Cum-Electrolyte for Supercapacitor*, Journal of The Electrochemical Society, **164**(13), pp. E379-E384, 2017.
- [24] Deng, L., Young, R.J., Kinloch, I.A., Abdelkader, A.M., Holmes, S.M., Rio, D.A.D.H. & Eichhorn, S.J., *Supercapacitance from Cellulose and Carbon Nanotube Nanocomposite Fibers*, ACS Applied Materials & Interfaces, **5**(20), pp. 9983-9990, 2013.
- [25] Islam, M.S., Ang, B.C., Andriyana, A. & Afifi, A.M., *A Review on Fabrication of Nanofibers via Electrospinning and Their Applications*, Springer Nature Applied Sciences, **1**(10), 1248, Oct. 2019.
- [26] Cheng, F., Yang, X., Zhang, S. & Lu W., *Boosting the Supercapacitor Performances of Activated Carbon with Carbon Nanomaterials*, Journal of Power Sources, **450**, 227678, Feb. 2020.
- [27] Yang, H., Kannappan, S., Pandian, A.S., Jang, J.H., Lee, Y.S. & Lu, W., *Graphene Supercapacitor with Both High Power and Energy Density*, Nanotechnology, **28**(44), 445401, Nov. 2017.
- [28] Yardimci, A.I., Kayhan, M., Durmus, A., Aksoy, M. & Tarhan, O., *Synthesis and Air Permeability of Electrospun PAN/PVDF Nanofibrous Membranes*, Research on Engineering Structures & Materials, **8**(2), pp. 223-231, 2022.

- [29] Karim, S.A., Mohamed, A., Abdel-Mottaleb, M.M., Osman, T.A. & Khattab, A., *Mechanical Properties and the Characterization of Polyacrylonitrile/Carbon Nanotube Composite Nanofiber*, Arabian Journal for Science and Engineering, **43**(9), pp. 4697-4702, Sep. 2018.
- [30] Song, Y., Wang, Y., Xu, L. & Wang, M., *Fabrication and Characterization of Electrospun Aligned Porous PAN/Graphene Composite Nanofibers*, Nanomaterials, **9**(12), 1782, Dec. 2019.
- [31] Mohamed, A., Yousef, S., Abdelnabyd, M.A., Osman, T.A., Hamawandi, B., Toprak, M.S., Muhammed, M. & Uheida, A., *Photocatalytic Degradation of Organic Dyes and Enhanced Mechanical Properties of PAN/CNTs Composite Nanofibers*, Separation and Purification Technology, **182**, pp. 219-223, Jul. 2017.
- [32] Phan, D.N., Dorjjugder, N., Saito, Y., Taguchi, G., Lee, H., Lee, J.S. & Kim, I.S., *The Mechanistic Actions of Different Silver Species at the Surfaces of Polyacrylonitrile Nanofibers Regarding Antibacterial Activities*, Materials Today Communications, **21**, 100622, Dec. 2019.
- [33] Wortmann, M., Frese, N., Mamun, A., Trabelsi, M., Keil, W., Buker, B., Javed, A., Tiemann, M., Moritzer, E., Ehrmann, A., Hutten, A., Schmidt, C., Golzhauser, A., Husgen, B. & Sabantina, L., *Chemical and Morphological Transition of Poly(acrylonitrile)/Poly(vinylidene Fluoride) Blend Nanofibers during Oxidative Stabilization and Incipient Carbonization*, Nanomaterials, **10**(6), 1210, Jun. 2020.
- [34] Zahari, A.M., Yusoff, A.R.M., Buang, N.A., Satishkumar, P., Jasni, M.J.F. & Yusop, Z., *Fabrication and Characterization of Polyvinylidene Fluoride Composite Nanofiber Membrane for Water Flux Property*, Jurnal Teknologi, **74**(11), pp. 9-14, Jun. 2015.
- [35] Karbownik, I., Rumijowska, O.R., Tobiła, M.F., Rybicki, T. & Tetrycz, H., *The Preparation and Characterization of Polyacrylonitrile-Polyaniline (PAN/PANI) Fibers*, Materials, **12**(4), 664, Feb. 2019.
- [36] Mohamed, A., Ghobara, M.M., Abdelmaksoud, M.K. & Mohamed, G.G., *A Novel and Highly Efficient Photocatalytic Degradation of Malachite Green Dye via Surface Modified Polyacrylonitrile Nanofibers/Biogenic Silica Composite Nanofibers*, Separation and Purification Technology, **210**, pp. 935-942, Feb. 2019.
- [37] Li, J. H., Zhang, H., Zhang, W. & Liu, W., *Nanofiber Membrane of Graphene Oxide/Polyacrylonitrile with Highly Efficient Antibacterial Activity*, Journal of Biomaterials Science, Polymer Edition, **30**(17), pp. 1620-1635, Nov. 2019.
- [38] Yang, L., Yang, L., Xu, G., Feng, Q., Li, Y., Zhao, E., Ma, J., Fan, S. & Li, X., *Separation and Recovery of Carbon Powder in Anodes from Spent Lithium-Ion Batteries to Synthesize Graphene*, Scientific Reports, **9**(1), 9823, Dec. 2019.
- [39] Yalcinkaya, F., Yalcinkaya, B., Pazourek, A., Mullerova, J., Stuchlik, M. & Maryska, J., *Surface Modification of Electrospun PVDF/PAN Nanofibrous Layers by Low Vacuum Plasma Treatment*, International Journal of Polymer Science, 2016, pp. 1-9, 2016.
- [40] Elkhaldi, R.M., Guclu, S. & Koyuncu, I., *Enhancement of Mechanical and Physical Properties of Electrospun PAN Nanofiber Membranes Using PVDF Particles, Desalination and Water Treatment*, **57**(54), pp. 26003-26013, Nov. 2016.
- [41] Arthi, R., Jaikumar, V. & Muralidharan, P., *Development of Electrospun PVDF Polymer Membrane as Separator for Supercapacitor Applications*, Energy Sources, Part A: Recovery, Utilization, and Environmental Effects, **44**(1), pp. 2294-2308, Mar. 2022.
- [42] Notodarmojo, S., Sugiyana, D., Handajani, M., Kardena, E. & Larasati, A., *Synthesis of TiO<sub>2</sub> Nanofiber-Nanoparticle Composite Catalyst and Its Photocatalytic Decolorization Performance of Reactive Black 5 Dye from Aqueous Solution*, Journal of Engineering and Technological Sciences, **49**(3), pp. 340-356, Aug. 2017.
- [43] Yanilmaz, M., *Evaluation of Electrospun PVA/SiO<sub>2</sub> Nanofiber Separator Membranes for Lithium-Ion Batteries*, The Journal of The Textile Institute, **111**(3), pp. 447-452, Mar. 2020.
- [44] Costa, C.M., Silva, M.M. & Méndez, S.L., *Battery Separators Based on Vinylidene Fluoride (VDF) Polymers and Copolymers for Lithium Ion Battery Applications*, Royal Society of Chemistry Advances, **3**(29), 11404, 2013.
- [45] Zhong, C., Deng, Y., Hu, W., Qiao, J., Zhang, L. & Zhang, J., *A Review of Electrolyte Materials and Compositions for Electrochemical Supercapacitors*, Chemical Society Reviews, **44**(21), pp. 7484-7539, 2015.
- [46] Fang, D., Yan, B., Agarwal, S., Xu, W., Zhang, Q., He, S. & Hou, H., *Electrospun Poly[Poly(2,5-Benzophenone)]Bibenzopyrrolone/Polyimide Nanofiber Membrane for High-Temperature and Strong-Alkali Supercapacitor*, Journal of Materials Science, **56**(15), pp. 9344-9355, May 2021.

- [47] Rajeevan, S., John, S. & George, S.C., *Polyvinylidene Fluoride: A Multifunctional Polymer in Supercapacitor Applications*, Journal of Power Sources, **504**, 230037, Aug. 2021.
- [48] Diantoro, M., Istiqomah, I., Fath, Y.A., Mufti, N., Nasikhudin, N., Mevasana, W. & Alias, Y. B., *Hierarchical Activated Carbon–MnO<sub>2</sub> Composite for Wide Potential Window Asymmetric Supercapacitor Devices in Organic Electrolyte*, Micromachines, **13**(11), 1989, Nov. 2022.
- [49] Deka, B.K., Hazarika, A., Kim, J., Park, Y.B. & Park, H.W., *Recent Development and Challenges of Multifunctional Structural Supercapacitors for Automotive Industries: Review on Multifunctional Structural Supercapacitors*, International Journal of Energy Research, **41**(10), pp. 1397-1411, Aug. 2017.
- [50] Hwang, J.Y., Li, M., El-Kady, M.F. & Kaner, R.B., *Next-Generation Activated Carbon Supercapacitors: A Simple Step in Electrode Processing Leads to Remarkable Gains in Energy Density*, Advanced Functional Materials, **27**(15), 1605745, 2017.
- [51] Miao, J., Miyauchi, M., Simmons, T.J., Dordick, J.S. & Linhardt, R.J., *Electrospinning of Nanomaterials and Applications in Electronic Components and Devices*, Journal of Nanoscience and Nanotechnology, **10**(9), pp. 5507-5519, Sep. 2010.
- [52] Diantoro, M., Luthfiyah, I., Istiqomah, Widodo, H., Utomo, J. & Meevasana, W., *Electrochemical Performance of Symmetric Supercapacitor Based on Activated Carbon Biomass TiO<sub>2</sub> Nanocomposites*, Journal of Physics Conference Series, **2243**(1), 012077, Jun. 2022.